1.5-μm-Band Wavelength Conversion Based on Cascaded Second-Order Nonlinearity in $LiNbO_3$ Waveguides

M. H. Chou, I. Brener, M. M. Fejer, E. E. Chaban, and S. B. Christman

***Abstract*— We report wavelength conversion and spectral inversion using cascaded second-order nonlinearity in periodically poled $LiNbO_3$ waveguides pumped at 1.5 μm. The converter has an internal conversion efficiency of -8 dB, a conversion bandwidth of 76 nm, and a constant conversion efficiency for the 50-dB range of signal powers tested.**

***Index Terms*—Nonlinear optics, optical fiber communications, optical frequency conversion, wavelength conversion, wavelength-division multiplexing.**

WAVELENGTH conversion is an important function in wavelengt-division-multiplexed (WDM) optical networks. Among numerous demonstrated wavelength conversion techniques, difference frequency generation (DFG) [1] is attractive in several respects: it is an instantaneous process that easily accommodates more than terahertz modulation bandwidths, can simultaneously up and down convert multiple channels with equal efficiencies, has negligible spontaneous emission noise and has no intrinsic frequency chirp.

DFG-based wavelength converters have been demonstrated in AlGaAs [1], [2] and $LiNbO_3$ waveguides [3]–[5], showing promising results for WDM wavelength conversion. However, the use of DFG and current device efficiencies indictate the need for a single mode pump laser with ~50–100 mW of power operating in the 750–800-nm range. Moreover, it is difficult to simultaneously launch the 780-nm pump and 1.5-μm band signals into the fundamental mode of the waveguide, although this has been solved using an integrated mode coupling structure [4] In this letter, we demonstrate wavelength conversion in $LiNbO_3$ waveguides using a cascaded second-order nonlinearity $(\chi^{(2)} : \chi^{(2)})$ [6]–[8], where both the input pump and signals are in the 1.5-μm band. Mode matching in this case is simplified compared to DFG pumped at 780 nm, since all input wavelengths are in the same band and can be launched into a single port.

The $\chi^{(2)} : \chi^{(2)}$-based device for 1.5-μm band wavelength conversion uses a pump in the 1550-nm region. The pump at frequency ω_p is upconverted to frequency $2\omega_p$ by second-harmonic generation (SHG) via the second-order nonlinearity $\chi^{(2)}$. The generated $2\omega_p$ simultaneously mixes with input signals ω_s to generate wavelength shifted outputs $\omega_{\text{out}} = 2\omega_p - \omega_s$ by DFG via another $\chi^{(2)}$ process. Phasematching between interacting waves for both SHG and DFG is required, and this can be accomplished by choosing an appropriate quasi-phasematching (QPM) grating period. It is interesting to note that this $\chi^{(2)} : \chi^{(2)}$ process mimics four-wave mixing (FWM) which uses the third-order nonlinearity $\chi^{(3)}$. The effective $\chi^{(3)}$ of such process in $LiNbO_3$ under quasiphase-matching condition is 10^4–10^5 times larger than that of silica glass. The $\chi^{(2)} : \chi^{(2)}$ allows the use of a very short sample when compared to fiber, and has better noise figure compared to FWM in semiconductor optical amplifiers. The converted output is related to pump power and input signal power in the low conversion efficiency approximation by [7]

$$P_{\text{out}} \approx \tfrac{1}{4}\eta^2 L^4 P_p^2 P_s \tag{1}$$

where P_{out}, P_p, and P_s are converted output power, pump power and signal power, respectively. η is the normalized efficiency (the same for SHG and near degenerate DFG) in units of $\text{mW}^{-1}\cdot\text{cm}^{-2}$ (this number is proportional to both the mode overlap between the interacting waves and the material nonlinearity $\chi^{(2)}$), and L is the interaction length. The conversion efficiency scales with the fourth power of the interaction length, so doubling the device length will increase the conversion efficiency by a factor of 16. In the high-conversion efficiency regime, the exponent of L in 1 is less than 4 due to pump depletion. In an optimized $LiNbO_3$ waveguide with a normalized efficiency of 150%/W$\cdot$cm^2 (or 0.0015 $\text{mW}^{-1}\cdot\text{cm}^{-2}$) and 6-cm interaction length, one can achieve 0-dB conversion efficiency with ~75 mW of pump power; or 3-dB gain with ~100 mW of pump power.

We fabricated the waveguides by annealed proton exchange in periodically poled $LiNbO_3$ (PPLN) [9]. The device used in this experiment is 4 cm long, has a QPM period of 15 μm, waveguide width of 12 μm, proton exchange depth of 0.7 μm, and was annealed for 26 h at 325 °C. The above parameters allow phasematching at room temperature between the fundamental mode of the pump at 1556 nm and the fundamental mode of SHG wave at 778 nm. We can tune the pump wavelength by using waveguides with different QPM period and/or temperature tuning. The normalized efficiency of this device is 65%/W$\cdot$cm^2. One can achieve a normalized efficiency of 150%/W$\cdot$cm^2 by optimizing the mode overlap

Manuscript received November 24, 1998; revised February 16, 1999. This work was supported by the Office of Naval Research through JSEP, by Lucent Technologies, and by the Defense Advanced Research Projects Agency through the CNOM at Stanford University, Stanford, CA.

M. H. Chou and M. M. Fejer are with E. L. Ginzton Laboratory, Stanford University, Stanford, CA 94305-4085 USA.

I. Brener, E. E. Chaban, and S. B. Christman are with Bell Laboratories, Lucent Technologies, Murray Hill, NJ 07974 USA.

Publisher Item Identifier S 1041-1135(99)04221-4.

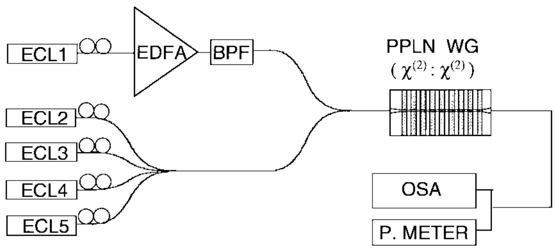

Fig. 1. Experimental setup. ECL: External cavity laser. BPF: Bandpass filter. PPLN WG: Periodically poled $LiNbO_3$ waveguide. OSA: Optical spectrum analyzer. The waveguide is fiber coupled at both the input and the output. The later is analyzed by an OSA and power meter.

between the fundamental mode of the pump and the first high-order mode of the second harmonic. At the input and output of this device, the waveguides are optimized for fiber coupling by tapering a section of 1-mm length to adiabatically transform the modes into and out of the wavelength conversion sections.

Fig. 1 shows a schematic diagram of the experimental setup used in this work. The pump laser is an external cavity laser (ECL) amplified by an erbium-doped fiber amplifier (EDFA) to a level of ~300 mW and filtered through a FBG in order to supress the amplified spontaneous emission (ASE). This pump is combined with signal sources generated in four different ECL's and fiber launched into the waveguides. The output of the waveguide is fiber coupled and later analyzed in an optical spectrum analyzer (OSA) and power meter. The fiber to fiber coupling loss in this configuration is ~4.5 dB due to reflection losses at the uncoated endfaces (~1.7 dB), mode mismatching between the fibers and the waveguide (~1.3 dB), and intrinsic waveguide losses (~1.5 dB, i.e., ~0.35 dB/cm).

We first characterized the device by measuring the SHG power versus pump wavelength. We chose to keep the waveguide at 90 °C (or higher) in order to avoid photorefractive effects. This effectively shifts the phasematching wavelength to 1562 nm, but keeps the other parameters unchanged. The device shows a near-ideal sinc^2 wavelength tuning curve with a peak internal efficiency (output SHG power divided by square of input pump power) of ~500%/W and an FWHM of ~0.27 nm at low pump power. At higher pump power (>100 mW), the device displayed a distorted wavelength tuning curve due to photorefractive effects of the generated second-harmonic waves, which results in waveguide nonuniformity and reduces the effective device length.

We performed simultaneous multichannel wavelength conversion with a pump power of ~110 mW launched inside the waveguide; the results, in Fig. 2, show that the efficiencies are the same (−15 dB) for all the input channels. The best conversion efficiency (−8 dB) was obtained with a pump power of ~175 mW in a similar device with a slightly different QPM period and operated at 120 °C, as shown in the inset of Fig. 2.

For $\chi^{(2)} : \chi^{(2)}$-based wavelength converters, the converted electric field is the complex conjugate of signal electric field, meaning that the output electric field spectrum is the mirror image of input spectrum about the pump wavelength. We show the spectral inversion properties of our device in Fig. 3 using an asymmetric input spectrum, formed by combining an ECL

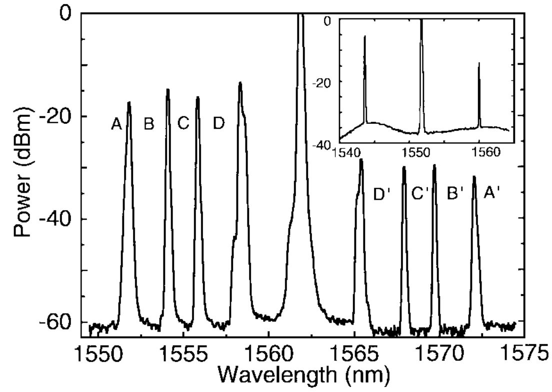

Fig. 2. Simultaneous wavelength conversion of four WDM channels with the same conversion efficiencies. Pump power is ~110 mW inside the PPLN waveguide at a wavelength of 1562 nm. The inset shows a −8-dB conversion efficiency of a similar device operated at 120 °C with 175 mW of pump power.

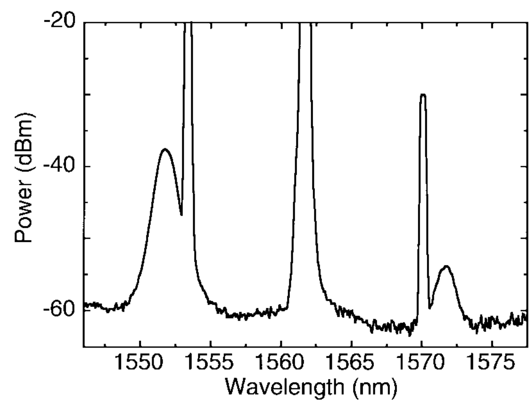

Fig. 3. Spectral inversion of the $\chi^{(2)} : \chi^{(2)}$ wavelength converter. The output electric field spectrum is the mirror image of input spectrum about the pump wavelength, a feature that can be used to invert the signal chirp.

signal and filtered ASE from an EDFA. This feature can be used to invert the signal chirp for dispersion management in a transmission system.

Fig. 4 shows the measured bandwidth of this wavelength converter when tuning the input signal wavelength while keeping the pump wavelength fixed at 1562 nm. This device has a 3-dB signal bandwidth of 76 nm, which is wider than the theoretical bandwidth of an ideal 4-cm-long device due to photorefractive effects at high pump powers.

We tested the linearity of this wavelength converter by varying the input signal power, as shown in Fig. 5. We measure a linear response for more than 50 dB with a maximum input signal power of ~0 dBm. The only saturation mechanism in this device comes from the depletion of SHG or pump power. We estimate a 0.16-dB deviation from linearity for a input power of 0 dBm in an ideal 6-cm-long device with a normalized efficiency of 150%/W·cm^2 and pump power of ~100 mW. For a device with a 2.5-cm interaction length, a normalized efficiency of 65%/W·cm^2, and pumped by ~100 mW, the deviation at 0-dBm signal power should be 0.006 dB, which is smaller than the resolution in this experiment. Our measurements confirm these estimates.

The conversion efficiency of this device currently is limited by photorefractive effects at high pump powers, which can

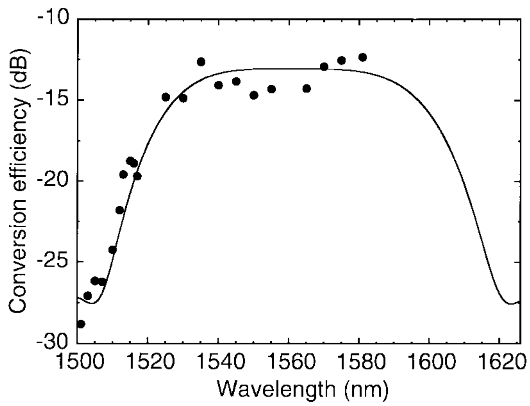

Fig. 4. Conversion efficiency vs. input signal wavelength. The closed circles are the measured results and the solid line is a theoretical fit to a device with an effective interaction length of 2.5 cm. The 1562-nm pump has a power of $\sim$135 mW inside the waveguide.

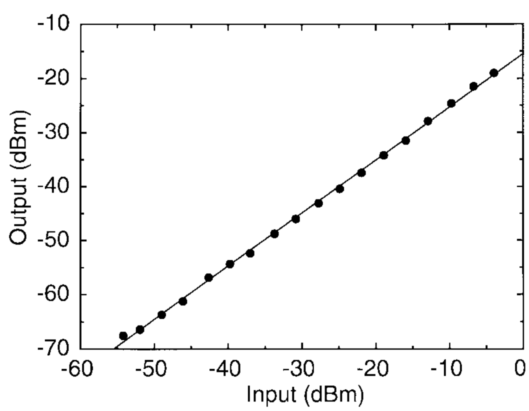

Fig. 5. Single-channel output/input transfer curve of the $\chi^{(2)} : \chi^{(2)}$ wavelength converter. This device has a linear response for more than 50-dB range of input signal powers.

be reduced by operating at higher temperature or annealing samples in an O_2 atmosphere. In addition, it has been shown that MgO:$LiNbO_3$ has several orders of magnitude more resistance to photorefractive effects than congruent $LiNbO_3$, and thus a similar device fabricated on MgO:$LiNbO_3$ would operate more efficiently.

In summary, we have demonstrated wavelength conversion within the 1.5-μm band using $\chi^{(2)} : \chi^{(2)}$ in PPLN waveguides. This approach requires only lasers operating in the 1550-nm region. We have shown spectral inversion and simultaneous conversion of four WDM channels, a static internal conversion efficiency of -8 dB, a conversion bandwidth of 76 nm, and a linearity over an input power range of more than 50 dB. With further improvements, a wavelength converter with 0-dB conversion efficiency or even gain is a feasible goal. In addition, this $\chi^{(2)} : \chi^{(2)}$-based wavelength converter can also function as clock recovery or time gating component by use of a pulsed pump.

ACKNOWLEDGMENT

The authors thank Crystal Technology for donating $LiNbO_3$ substrates and B. Eggleton for providing the fiber Bragg grating.

REFERENCES

[1] S. J. B. Yoo, "Wavelength conversion technologies for WDM network applications," *J. Lightwave Technol.*, vol. 14, pp. 955–966, 1996.

[2] S. J. B. Yoo, M. A. Koza, C. Caneau, and R. Bhat, "Simultaneous wavelength conversion of 2.5-Gbit/s and 10-Gbit/s signal channels by difference-frequency generation in an AlGaAs waveguide," in *1998 OSA Tech. Dig. Ser., Conf. Optical Fiber Communications*, vol. 2, paper WB5.

[3] C. Q. Xu, H. Okayama, and M. Kawahara, "1.5 μm band efficient broadband wavelength conversion by difference frequency generation in a periodically domain-inverted $LiNbO_3$ channel waveguide," *Appl. Phys. Lett.*, vol. 63, pp. 3559–3561, 1993.

[4] M. H. Chou, J. Hauden, M. A. Arbore, and M. M. Fejer, "1.5-μm-band wavelength conversion based on difference-frequency generation in $LiNbO_3$ waveguides with integrated coupling structures," *Opt. Lett.*, vol. 23, pp. 1004–1006, 1998.

[5] C. Q. Xu, H. Okayama, and T. Kamijoh, "$LiNbO_3$ quasiphasematched wavelength converter and its module," in *Proc. Eur. Conf. Optical Communications*, 1998, pp. 173–174.

[6] K. Gallo, G. Assanto, and G. Stegeman, "Efficient wavelength shifting over the erbium amplifier bandwidth via cascaded second order processes in lithium niobate waveguides," *Appl. Phys. Lett.*, vol. 71, pp. 1020–1022, 1997.

[7] G. P. Banfi, P. K. Datta, V. Degiorgio, and D. Fortusini, "Wavelength shifting and amplification of optical pulses through cascaded second-order processed in periodically poled lithium niobate," *Appl. Phys. Lett.*, vol. 7, pp. 136–138, 1998.

[8] G. I. Stegeman, D. J. Hagan, and L. Toner, "$\chi^{(2)}$ cascading phenomena and their applications to all-optical signal processing, mode-locking, pulse compression and solitons," *Opt. Quantum Electron.*, vol. 28, pp. 1691–1740, 1996.

[9] L. E. Myers, R. C. Eckardt, M. M. Fejer, R. L. Byer, W. R. Bosenberg, and J. W. Pierce, "Quasiphase-matched optical parametric oscillators in bulk periodically poled $LiNbO_3$," *J. Opt. Soc. Amer. B*, vol. 12, pp. 2102–2106, 1995.